Worcester Polytechnic Institute

Department of Chemistry and Biochemistry

Phosholipase Cβ interacts with Argonaute 2 in stress granules to change the microRNAs population in response to osmotic stress

A Thesis in

Biochemistry

by

Ashima Singla

Submitted in Partial Fulfillment of the

Requirements for the Degree of

Master of Science

DECEMBER 2017

Ashima Singla

We, the dissertation committee for the above candidate for the

Masters in Science degree, hereby recommend

acceptance of this dissertation.

Dr. Suzanne Scarlata – Thesis Advisor

Professor, Department of Chemistry and Biochemistry

Dr. Arne Gericke – Thesis Committee Member

Professor, Department of Chemistry and Biochemistry

Dr. Carissa Olsen – Thesis Defense Member

Professor, Department of Chemistry and Biochemistry

This dissertation is accepted by the Graduate School

Dr. Terri Camesano

Dean of the Graduate Studies

Abstract of the Dissertation

Phosholipase Cβ interacts with argonaute 2 in stress granules to change the microRNAs population in response to osmotic stress

by

Ashima Singla

Masters of Science

in

Biochemistry

Department of Chemistry and Biochemistry

Worcester Polytechnic Institute

December 2017

When cells are exposed to environmental stress, they respond by compartmentalizing mRNA and translation proteins in stress granulates to protect mRNA. However, the mechanism through which external stress is communicated into the cell to form stress granules is unknown. Phospholipase Cβ (PLCβ) is activated by Gαq on the plasma membrane in response to sensory stimuli to initiate calcium signals resulting in a variety of cellular responses. Here, we show that PLCβ binds to major proteins that organize stress granules as well as the main component of the RNA-induced silencing machinery, Argonaute-2 (Ago2). Under stress, PLCβ moves from the plasma membrane to the cytosol to escort Ago2 into stress granules and potentially inhibit mRNA degradation by regulating microRNAs (miRs) expression. Using a model muscle cell line functionally adapted to handle stress, we find that upon osmotic stress, the movement of PLCβ into the cytosol into stress granules changes the population and distribution of miRs, and in particular, members of the *let* family. The impact of changes in *let* is to acutely affect glucose

metabolism allowing cells to adapt to stress conditions. Our studies present a model in which PLCβ relays information about external stress to promote stress granule formation and protect mRNAs. Some this dissertation are based on collaborative work of Ashima Singla (dissertation author), Dr. Yuanjian Guo, Stony Brook University and Dr. Osama Garwain, Worcester Polytechnic Institute. Experiments for Figure 2.12, 2.13, 2.14 and Table 3 were done by Dr. Yuanjian Guo, experiment for Table 3 was done by Osama Garwain, rest of the figures and tables were done by Ashima Singla (dissertation author).

Dedication Page

I dedicate this work to my parents Sushil Kumar Singla and Ravi Singla, my brother Gautam Singla and my sister-in law Antarpreet Kaur Singla as it would not have been possible without them.

Table of Contents

List of Figures

List of Tables

List of Abbreviations

AGO2 Argonaute 2

C3PO Component 3 Promoter of RISC

CTD C- terminal domain

DAG Diacylglycerol

eGFP enhanced green fluorescent protein

ER Endoplasmic reticulum

eYFP enhanced yellow fluorescent protein

FCS Fluorescence Correlation Spectroscopy

FLIM Fluorescence Lifetime Imaging

FRET Förster Resonance Energy Transfer

GPCR G-protein coupled receptor

IP3 Inositol-1,4,5- trisphosphate

mRNA messenger RNA

miRNA micro RNA

PH Pleckstrin homology

PIP2 Phosphotidylinositol-4,5-bisphosphate

PLC Phospholipase C

PLCβ Phospholipase C β

PLCβ1 Phospholipase C β1

RISC RNA induced silencing complex

RNAi RNA interference

siRNA small interfering RNA

SGs stress granules

TRAX Translin- associated factor X

ACKNOWLEDGEMENTS

It would like to thank many people from whom I have learnt tremendously over the past two years and who made this thesis possible with their never-ending support and encouragement.

Foremost, I would like to express my sincere gratitude to my advisor Dr. Suzanne Scarlata for her continuous support and the opportunity to carry out the research. She is the best advisor a graduate student ask could for. I am grateful to her for her never ending support, openness, motivation and immense knowledge in every field. She has been a great mentor to me. I am thankful to her for her unwavering faith in everything I did. Her guidance has not only helped me do my research, but also become a better person. I will always look up to her as my woman scientist role model.

I would also like to thank the other members of my committee. Dr. Arne Gericke for numerous insightful conversations that I had with him, creating a wonderful and collaborative lab space to carry out my research and his encouragement throughout my academic and research career. Dr. Carissa Olsen for conducting an intensive scientific writing seminar which has helped me hone my written skills and her support.

I would like to thank all the wonderful group members of the Scarlata Lab for providing an extremely friendly and stimulating research environment. I am especially grateful to Osama Garwain for his constant support throughout my research and his friendship. One of the experiments presented in this dissertation was performed by him. I am extremely grateful to Sid, Andrea, Kaitlyn and Kate for their help in research as well as for being great friends. I am very thankful to everyone for their support and inspiration. I would also like to thank the previous lab members- Dr. Urszula Golebiewska, Dr. Yuanjian Guo and Dr. Shriya Sahu for their suggestions

and readiness to help me. I would like to thank all the undergraduate students I worked with Samantha, Sam, Cory and Chris for helping me to be a better teacher. The last two years were so much fun because of all of my lab members. Thanks to everyone for being there.

I would like to thank members of Gericke Lab their support in the last two years. I would like to thank them for letting me use their lab space and equipment for my experiments. I would like especially like to thank Anne Marie Bryant for being the amazing person she is. My life would have been so different if I hadn't met her. I would like to thank her for teaching me protein purification, for countless scientific discussions and most importantly her friendship. I am grateful to her for helping me through difficult times and always being there for me.

I would like to thank Dr. William Kobertz from UMass Medical School, Worcester and his then postdoc Kevin O'Brien for having me over in their lab and teaching me how to perform the methionine/cysteine incorporation experiment. I would like to acknowledge Dr. John Leszyk, Mass Spectrometry facility, UMass Medical School for his help with proteomics study. I am very grateful to everyone in the Department of Chemistry and Biochemistry, especially Ann Mondor, and Paula Moravek their support.

I would like express my sincerest gratitude to my parents for making me who I am. I thank them for their selfless love, support and faith in everything I do. I am very thankful to my brother and my sister-in-law for their constant support and encouragement. I am very fortunate to have them in my life. Lastly, I thank all my friends and other family members their support and best wishes.

CHAPTER I – GENERAL INTRODUCTION

Phospholipase C β

Phospholipase C (PLC) enzymes are phosphoinositide specific signaling enzymes that catalyze the hydrolysis of the membrane phospholipid phosphotidylinositol-4,5-bisphosphate (PIP_2) into inositol-1,4,5-trisphosphate (IP_3) and diacylglycerol (DAG). IP_3 and DAG act as second messengers for many signaling processes [1-3]. IP_3 traverses through the cytoplasm and binds to receptors in the endoplasmic reticulum (ER) resulting in the release of Ca^{2+} from the ER lumen. The released Ca^{2+} along with DAG on the plasma membrane activate protein kinase C (PKC) which triggers a downstream signaling cascade leading to various cellular and physiological events such as cell growth and proliferation, differentiation, chemotaxis, muscle contraction and neurotransmission [4, 5] . Years of evolution has led to six families of PLCs PLCβ, PLCγ, PLCδ, PLCε, PLCζ and PLCη with a specific mode of regulation. Further differential splicing of these PLCs' pre-mRNAs lead up to 30 PLC enzymes. PLC isozymes share a conserved core structure but differ in protein domain arrangement, activation pathways and tissue distribution. The catalytic core of PLC comprises of the N-terminal pleckstrin homology (PH) domain which helps with the binding to the membrane, multiple EF hands, followed by the catalytic X and Y domain connected by a linker, and a C2 domain (Figure 1.1)

PLCβ1-4 have a ~400 amino acid long coiled-coil C-terminal tail/domain (CTD) after the C2 domain compared to the other PLC isozymes. CTD confers unique properties such as activation and regulation by Gαq, to the PLCβ enzymes [8]. The four PLCβ isozymes differ in their tissue distribution and ability to be activated by G proteins.

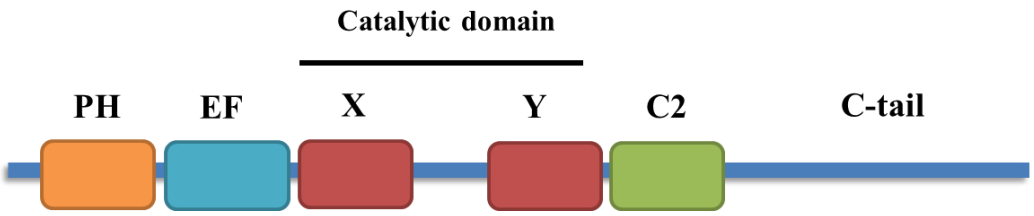

Figure 1.1- Schematic diagram of structural domains present in Phospholipase Cβ family.

Extracellular signaling hormones such as angiotensin, bradykinin, or neurotransmitters such as dopamine, acetylcholine and serotonin result in activation of PLCβ isozymes through the G-protein coupled receptor (GPCR) pathway (Figure 1.2) [9]. PLCβs bind to heterotrimeric G proteins Gαq, Gβ and Gγ in the cell membrane. Binding of a signaling ligand to a GPCR receptor triggers a conformational change in the GPCRs and activates the coupled G protein. Upon activation, Gαq stimulates PLCβ to catalyze the hydrolysis of PIP_2 into IP_3 and DAG which results in an increase of the intracellular calcium level and activation of PKC, respectively [10]. Thus, PLCβ helps relay the extracellular ligand binding event into an intracellular signaling pathway. This thesis focuses on PLCβ1, which is found in high levels in neuronal cells and is the most strongly activated by Gαq.

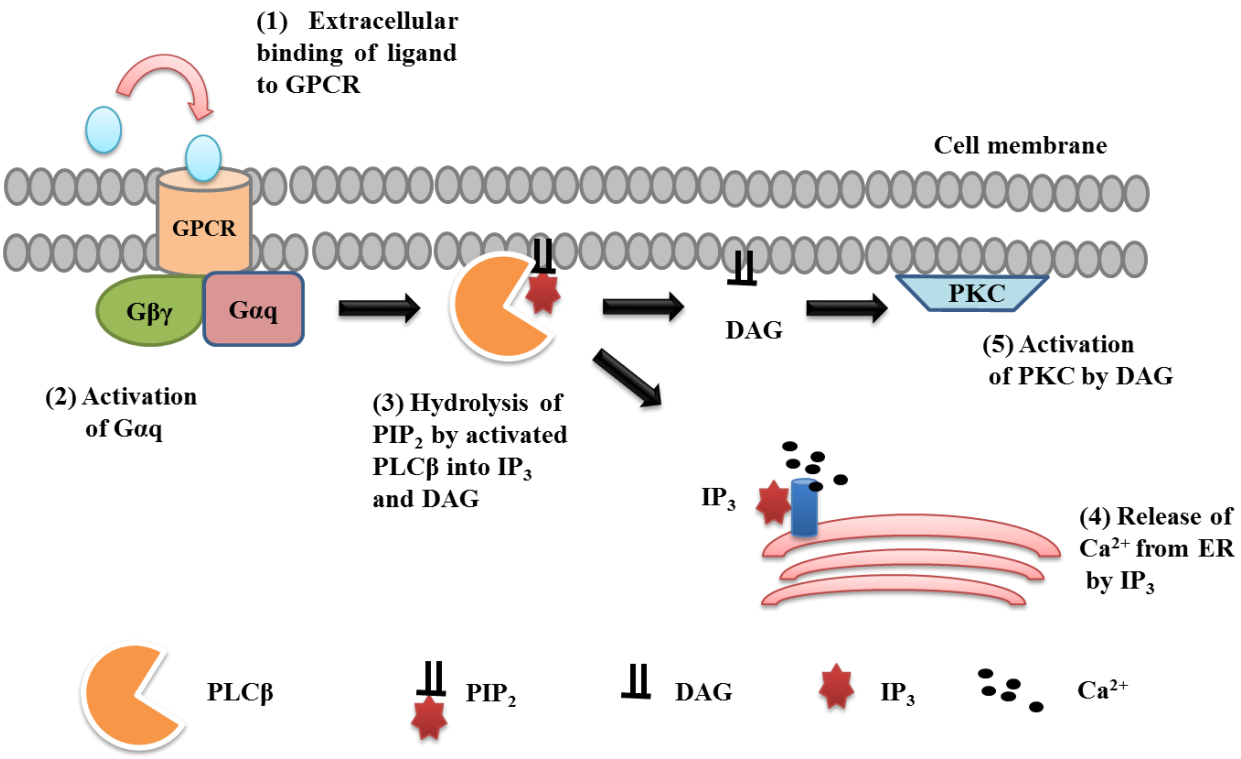

Figure 1.2- Cartoon representation of phospholipase C β (PLCβ) signaling pathway. The main steps of the pathway are illustrated. *Reprinted from Shriya Sahu's dissertation thesis* [27]

Chapter II

Phosholipase Cβ interacts with Argonaute 2 in stress granules to change the microRNA population in response to osmotic stress

Introduction

Cells have adopted many mechanisms to communicate with their external environment and to determine the optimal conditions for growth, to move or to carry out their particular function [11]. When conditions become adverse, cells will halt the production of proteins to conserve energy until the stress is relieved [11]. Stress granules (SGs) are part of a conserved cellular stress response and are implicated in the pathogenesis of various diseases such as cancer, neurodegeneration, and viral infections [12]. SGs are 100-200 nm sized membrane-less aggregates of stalled translation complexes, and are composed of non-translating mRNAs, translation initiation complexes, poly (A)-binding protein, and many additional mRNA related proteins [12]. Stress granules appear when cells are subjected to environmental stressors like heat shock, toxic molecules such as arsenite, oxidative stress, hypo-or hyper-osmolarity, UV irradiation and nutrient deprivation. Stress granules are thought to act as a "juncture" to protect non-translated mRNAs from degradation until the stress is removed. SGs are distinct from processing bodies (P-bodies) that store and process mRNA, Although SGs are most commonly formed under external stress conditions, SG have also been observed under non-stress conditions and can act as waiting stations that allow cells to decide whether mRNAs need to be degraded, stored or enter the translational machinery [13].

SGs have been proposed to recruit specific mRNA transcripts which may influence function [14]. Additionally, many proteins are thought to incorporate into stress granules which might depend on the stress conditions. One protein that is a hallmark of SGs is argonaute 2 (Ago2) [15]. Ago2 is the main nuclease component of the RNA-induced silencing complex (RISC) which degrades mRNA in response to different signals. RISC activity allow cells to rapidly and locally change the protein content without the need for changes in transcription [16].

Incorporation of Ago2 into SGs is likely to repress RISC activity. Recent studies have reported that cellular stress results in significant global remodeling of Ago2 binding across the transcriptome with trends towards enhanced binding of specific mRNAs [17]. It has been postulated that tighter interactions between Ago2-mRNA contributes to the translational repression of certain mRNAs during cellular stress while allowing productions of proteins required for relief of stress [17]. Thus, the formation and stability of stress granules may influence the local protein population, and local cell function through changes in Ago2 activity.

miRNAs play a key role in metabolic homeostasis by governing the response to alterations in cellular states [18]. For example, in neuronal cells, the upregulation of let-7 miRNA family inhibits glucose metabolism in the pancreas, liver, and muscle whereas Lin28 family overexpression results in insulin sensitivity, enhanced glucose tolerance, and resistance to diabetes [19].

Cell membranes contain many proteins that monitor the external environment. One important class of receptors is the G protein coupled receptor family that binds external ligands

and communicates this information to the cell interior allowing the cell to initiate an appropriate response [1-3]. Our lab studies signaling through Gαq-coupled GPCRs that activate phospholipase Cβ (PLCβ) resulting in calcium-induced responses leading to mitogenic and proliferative changes in the cell [2]. Even though the main substrate of PLCβ, phosphatidylinositol 4,5-bisphosphate, and its coupled G protein is concentrated on the plasma membrane, a significant portion of PLCβ is found in the cytosol. Several years ago, the Scarlata group reported that this cytoplasmic fraction can bind to a promoter of RNA-induced silencing, component 3 Promoter (C3PO) of RISC, and this binding can reverse RNA-induced silencing of specific genes [20]. Reversal of silencing was independent of PLCβ1's catalytic activity and the binding to C3PO occurs in a region distant from the active site [20]. Additionally, these and other studies indicated movement of PLCβ and increased colocalization with Ago2 with siRNA treatment suggesting that certain types of stress may enhance interactions between these proteins.

RISC activity has been found at synapses suggesting that it depends on local inputs [21, 22]. It is notable that PLCβ enzymes are highly expressed in neuronal cells, and we have previously obtained evidence that in smooth muscle cells, osmotic stress may redirect PLCβ from the plasma membrane to the cytosol. These observations prompted us to investigate whether PLCβ has a role in regulating local RISC activity under stress conditions.

Objectives of this thesis

The main questions that we try to answer in this dissertation work are-

1. What are the proteins that interact with PLCβ in the cytoplasm and how do they change under stress conditions?

2. How does the interaction of PLCβ1 with cytosolic proteins affect the Ca2+ signals mediated by PLCβ1 during stress?

3. How does PLCβ1 help cells adapt to stress conditions?

Here, we show that in neuronal cells stress causes PLCβ1 to move to the cytoplasm and bind to Ago2 as it moves into SGs. Moreover, we find that movement of PLCβ1 and Ago2 into SGs alters silencing RNAs that control glucose metabolism allowing the cells to rapidly adapt to stress. These studies indicate that PLCβ can act as a sensor to allow cells to monitor and respond to external inputs through SG formation and changes in RNA-induced silencing.

RESULTS

PLCβ1 binds to stress granule associated proteins. We have previously reported on a stable cytosolic population of PLCβ1 that interacts with proteins involved in the RNA-induced silencing machinery. [23-25]. To determine the cytosolic proteins that are associated with PLCβ1, we disrupted unsynchronized PC12 cells, removed the membrane fraction and nuclei, and isolated PLCβ1 with its associated proteins using a monoclonal antibody. We then eluted the complexes and identified the proteins by mass spectrometry. We find that ~30% of the total proteins in PLCβ1complexes are markers for stress granules (e.g.PABPC1, Fxr2, EIF4G1 and Ago2, see

Table 1), along with known partners of PLCβ (C3PO, α-synuclein). These data suggest that a population of PLCβ1 may be associating with stress granules.

32.1%	Known Stress Granule Proteins
8.35%	Ribosomal Proteins

Uniprot ID	Protein Name	Intensity Levels	% of total Spectra
A0A0G2JV65	14-3-3 protein zeta/delta, Ywhaz	990080	0.1648
A0A0G2JW88	Microtubule-associated protein, Map4	125640	0.0209
A0A0G2JYE0	Protein Atxn2l, Atxn2l	316410	0.0527
A0A0G2K8K0	Protein Sfpq, Sfpq	559700	0.0932
A0A0U1RS25	Protein Upf1, Upf1 4	1579100	0.2629
D3Z941	Protein Mars, Mars	696260	0.1159
D3ZC82	Protein Nufip2, Nufip2	18058	0.0030
D3ZPL1	Cleavage and polyadenylation specific factor 6, 68kDa (Predicted), isoform CRA_b, Cpsf6	9880500	1.6448
D3ZU13	Protein Eif4g1, Eif4g1	1178300	0.1961
D4AB03	Protein Fam120a, Fam120a	410640	0.0684
D4ADC2	Protein Helz2, Helz2	312960	0.0521
F1LMV6	Protein Dsp, Dsp	11775	0.0020
F1LPS8	Transcriptional activator protein Pur-alpha, Pura	403770	0.0672
F1LRP7	Protein argonaute-2, Ago2	17775	0.0030
F1LVV4	Protein Rcc2, Rcc2	53762	0.0089
F1M062	Protein Larp1, Larp1	406340	0.0676
G3V9N0	Polyadenylate-binding protein, Pabpc4	92555	0.0154
G3V9N1	RCG21137, Pgam5	258290	0.0430
M0R9X8	Cytoplasmic dynein 1 heavy chain 1, Dync1h1	967010	0.1610
O09032	ELAV-like protein 4, Elavl4	208370	0.0347
O88600	Heat shock 70 kDa protein 4, Hspa4	1459200	0.2429
P0CG51	Polyubiquitin-B, Ubb	5659000	0.9420
P28023	Dynactin subunit 1, Dctn1	139760	0.0233
P28480	T-complex protein 1 subunit alpha, Tcp1	170520	0.0284
P46462	Transitional endoplasmic reticulum ATPase, Vcp	970920	0.1616
P52296	Importin subunit beta-1, Kpnb1	37472	0.0062
P61980	Heterogeneous nuclear ribonucleoprotein K, Hnrnpk	26715	0.0044
P62828	GTP-binding nuclear protein Ran, Ran	2.51E+07	4.1829
P62909	40S ribosomal protein S3, Rps3	6910700	1.1504
P63245	Guanine nucleotide-binding protein subunit beta-2-like 1, Gnb2l1 /RACK1	252680	0.0421
P68255	14-3-3 protein theta, Ywhaq	1230600	0.2049
P82995	Heat shock protein HSP 90-alpha, Hsp90aa1	6442100	1.0724
P85834	Elongation factor Tu, mitochondrial, Tufm	171370	0.0285
Q1JU68	Eukaryotic translation initiation factor 3 subunit A, Eif3a 2	328760	0.0547
Q4G061	Eukaryotic translation initiation factor 3 subunit B, Eif3b	500320	0.0833

Q5XIF6	Tubulin alpha-4A chain, Tuba4a	7542300	1.2555
Q6P502	T-complex protein 1 subunit gamma, Cct3	26160	0.0044
Q91V33	KH domain-containing, RNA-binding, signal transduction-associated protein 1, Khdrbs1	98010	0.0163
Q9EPH8	Polyadenylate-binding protein 1, Pabpc1	1268600	0.2112
Q9EQV9	Carboxypeptidase B2, Cpb2 2	379250	0.0631
Q9QZA2	Programmed cell death 6-interacting protein, Pdcd6ip	279030	0.0464
A0A0G2K719	Protein Ddx3x, Ddx3x	1985300	0.3305
B1H2A6	Fxr2 protein, Fxr2	1358100	0.2261
Q3B8Q1	Nucleolar RNA helicase 2, Ddx21 2	166310	0.0277
Q5XI81	Fragile X mental retardation syndrome-related protein 1, Fxr1	1671100	0.2782
Q80WE1-2	Isoform 2 of Fragile X mental retardation protein 1 homolog, Fmr1	1405700	0.2340
Q641Y8	ATP-dependent RNA helicase DDX1, Ddx1	283930	0.0473
A0A0G2K2C7	Protein Usp9x, Usp9x	1.07E+08	17.7418
Q5M9G3	Caprin-1, Caprin1	1775300	0.2955
A0A0H2UHS7	60S ribosomal protein L18, Rpl18	3062000	0.5097
A0A0H2UHV4	Eukaryotic translation initiation factor 5B, Eif5b	161030	0.0268
B0BN81	40S ribosomal protein S5, Rps5	269540	0.0449
B2RYR8	40S ribosomal protein S8, Rps8 2	825130	0.1374
B5DFC8	Eukaryotic translation initiation factor 3 subunit C, Eif3c	401250	0.0668
D4A9D6	DEAH (Asp-Glu-Ala-His) box polypeptide 9 (Predicted), Dhx9	336240	0.0560
P18445	60S ribosomal protein L27a, Rpl27a	2292400	0.3816
P21531	60S ribosomal protein L3, Rpl3	191040	0.0318
P24049	60S ribosomal protein L17, Rpl17 2	2352600	0.3916
P24051	40S ribosomal protein S27-like, Rps27l	4511400	0.7510
P29314	40S ribosomal protein S9, Rps9	4917700	0.8186
P41123	60S ribosomal protein L13, Rpl13	1214600	0.2022
P62250	40S ribosomal protein S16, Rps16	2701200	0.4497
P62282	40S ribosomal protein S11, Rps11	641050	0.1067
P62703	40S ribosomal protein S4, X isoform, Rps4x 2	2703500	0.4500
P62832	60S ribosomal protein L23, Rpl23 2	4035600	0.6718
P62853	40S ribosomal protein S25, Rps25 2	3939400	0.6558
P62856	40S ribosomal protein S26, Rps26 3	4230900	0.7043
P62914	60S ribosomal protein L11, Rpl11	565190	0.0941
P83732	60S ribosomal protein L24, Rpl24 2	2450500	0.4079
Q5BJS0	Putative ATP-dependent RNA helicase DHX30, Dhx30	466570	0.0777
Q6P3V9	60S ribosomal protein L4, Rpl4	6012600	1.0009
Q6PDV7	60S ribosomal protein L10, Rpl10	1880700	0.3131

P08413	Calcium/calmodulin-dependent protein kinase type II subunit beta, Camk2b	126390	0.0210
Q66HD0	Endoplasmin, Hsp90b1	1965200	0.3271
A0A096MIX2	DEAD (Asp-Glu-Ala-Asp) box polypeptide 17, isoform CRA_a, Ddx17	1798900	0.2995
A0A096MKE9	DNA ligase, Lig3	14789	0.0025
A0A0A0MXX0	CD2-associated protein, Cd2ap	1.86E+07	3.0951
A0A0G2JSH5	Serum albumin, Alb	1.83E+07	3.0390
A0A0G2JSH6	Transient receptor potential cation channel subfamily V member 2, Trpv2	904190	0.1505
A0A0G2JT63	Protein Cyfip2, Cyfip2	22455	0.0037
A0A0G2JU96	Protein Ahnak, Ahnak	522160	0.0869
A0A0G2JUC9	Protein Herc2, Herc2	23490	0.0039
A0A0G2JUU7	Protein Tubgcp3, Tubgcp3	282130	0.0470
A0A0G2JVL8	Protein Iars, Iars	107810	0.0179
A0A0G2JWD6	AP-3 complex subunit beta, Ap3b1	772930	0.1287
A0A0G2JXJ7	Extended synaptotagmin-1, Esyt1	42850	0.0071
A0A0G2JXZ3	Transcriptional regulator ATRX, Atrx	2,319.40	0.0004
A0A0G2JYH7	Protein Sh2d3c, Sh2d3c	117250	0.0195
A0A0G2JZ52	Protein Hnrnpu, Hnrnpu	2990700	0.4978
A0A0G2JZI2	Protein Eprs, Eprs	294760	0.0491
A0A0G2JZY6	Protein Sptbn1, Sptbn1	32859	0.0055
A0A0G2K0B4	E3 ubiquitin-protein ligase NEDD4, Nedd4	299540	0.0499
A0A0G2K1Q9	Erythrocyte protein band 4.1-like 3, isoform CRA_e, Epb41l3	325520	0.0542
A0A0G2K2M9	Protein Srrm2, Srrm2	149320	0.0249
A0A0G2K2P5	Protein Tjp1, Tjp1	52438	0.0087
A0A0G2K3H2	Protein Dock7, Dock7	8,438.50	0.0014
A0A0G2K4Y7	Unconventional myosin-Va, Myo5a	818560	0.1363
A0A0G2K5A4	Uncharacterized protein 4	23887	0.0040
A0A0G2K5C6	Microtubule-associated protein 1A, Map1a	46183	0.0077
A0A0G2K6I4	Protein Enah, Enah	554530	0.0923
A0A0G2K6S9	Myosin-11, Myh11	349120	0.0581
A0A0G2K736	Protein Kdm1a, Kdm1a	15926	0.0027
A0A0G2K926	Protein LOC297568, LOC297568	1075300	0.1790
A0A0G2K9T1	E3 ubiquitin-protein ligase, Itch	888080	0.1478
A0A0G2KAL8	Short transient receptor potential channel 3, Trpc3 4	146450	0.0244
A0A0G2KB74	Protein Dip2a, Dip2a	212120	0.0353
A0A0U1RRP9	Protein C2, C2 4	3720900	0.6194
A3KNA0	Aqr protein, Aqr	166790	0.0278
A9UMV8	Histone H2A.J, H2afj 2	2893800	0.4817
B1WBU2	LOC682033 protein, Ppp2r3b 2	1642200	0.2734

B1WC16	BCL2-associated transcription factor 1, isoform CRA_a, Bclaf1	209850	0.0349
B2GUZ3	Mthfd1l protein, Mthfd1l	29176	0.0049
B2RYM3	Inter-alpha trypsin inhibitor, heavy chain 1 (Predicted), isoform CRA_a, Itih1	5706300	0.9499
B2RYP8	A disintegrin and metalloprotease domain 8 (Predicted), isoform CRA_b, Tubgcp2	182360	0.0304
B4F772	Heat shock 70 kDa protein 4L, Hspa4l	180360	0.0300
C0JPT7	Filamin alpha, Flna	13618	0.0023
D3ZAS8	Protein Sart3, Sart3	125360	0.0209
D3ZB81	Protein Slc25a31, Slc25a31 3	6287400	1.0466
D3ZD97	DEAH (Asp-Glu-Ala-His) box polypeptide 15 (Predicted), isoform CRA_b, Dhx15	601800	0.1002
D3ZFH5	Protein Itih2, Itih2	2781700	0.4631
D3ZFJ3	Protein Sh3bp1, Sh3bp1	5998800	0.9986
D3ZFP4	DNA helicase, Mcm3	159860	0.0266
D3ZH41	Cytoskeleton-associated protein 4 (Predicted), Ckap4	583380	0.0971
D3ZIE9	Protein Aldh18a1, Aldh18a1 3	1395400	0.2323
D3ZRK0	Protein Fam83h, Fam83h	357750	0.0596
D3ZUK4	Protein Trim33, Trim33	28931	0.0048
D3ZYD7	Protein Ccdc88a, Ccdc88a	18528	0.0031
D4A2D3	Protein Mycbp2, Mycbp2	32211	0.0054
D4A4J0	Protein Supt16h, Supt16h	890130	0.1482
D4A4Z9	Protein Ktn1, Ktn1	166520	0.0277
D4A507	Protein Clip3, Clip3	702910	0.1170
D4A857	Importin 9 (Predicted), Ipo9	409780	0.0682
D4A8A0	DNA fragmentation factor subunit beta, Cad	28853	0.0048
D4A8H8	Cytoplasmic FMR1 interacting protein 1 (Predicted), Cyfip1	48469	0.0081
D4AEG2	Protein Rab32, Rab32	920700	0.1533
E9PT22	Protein Inf2, Inf2	353460	0.0588
E9PU01	Protein Chd4, Chd4	33663	0.0056
F1LM33	Leucine-rich PPR motif-containing protein, mitochondrial, Lrpprc	140580	0.0234
F1LNF0	Protein Myh14, Myh14	125710	0.0209
F1LNR1	Protein Clasp1, Clasp1	122160	0.0203
F1LQS3	60S ribosomal protein L6, Rpl6-ps1 3	1390500	0.2315
F1LRI5	Protein Gcn1l1, Gcn1l1	11825	0.0020
F1LRL9	Microtubule-associated protein 1B, Map1b	274590	0.0457
F1LV13	Heterogeneous nuclear ribonucleoprotein M, Hnrnpm	240910	0.0401
F1LX07	Protein Slc25a12, Slc25a12	2029400	0.3378
F1LZW6	Protein Slc25a13, Slc25a13	973190	0.1620

F1M5M9	Protein Srgap3, Srgap3	137500	0.0229
F1M7P4	Peripherin, Prph	695540	0.1158
F1M953	Stress-70 protein, mitochondrial, Hspa9	2636500	0.4389
F7EYF1	E3 ubiquitin-protein ligase, Wwp2	899040	0.1497
G3V679	Transferrin receptor protein 1, Tfrc	109720	0.0183
G3V6L4	Kinesin-like protein, Kif5c	118680	0.0198
G3V6P7	Myosin, heavy polypeptide 9, non-muscle, Myh9	749910	0.1248
G3V6S8	Serine/arginine-rich splicing factor 6, Srsf6	287920	0.0479
G3V6T1	Coatomer subunit alpha, Copa	40235	0.0067
G3V7C6	Tubulin beta-4B chain, Tubb4b	7228200	1.2032
G3V7M0	Protein Cnot1, Cnot1	23422	0.0039
G3V8T4	DNA damage-binding protein 1, Ddb1	89699	0.0149
G3V918	Phosphoribosylglycinamide formyltransferase, isoform CRA_a, Gart	193930	0.0323
G3V9J1	Protein LOC297568, LOC297568	4992300	0.8310
G3V9Y1	Myosin, heavy polypeptide 10, non-muscle, isoform CRA_b, Myh10	423540	0.0705
M0R7B4	Protein LOC684828, LOC684828	3215100	0.5352
M0R7E6	Protein Srrt, Srrt	737920	0.1228
M0RBF1	Complement C3, C3	4450900	0.7409
O08629	Transcription intermediary factor 1-beta, Trim28	291620	0.0485
O35964	Endophilin-A2, Sh3gl1	2238900	0.3727
O55043	Rho guanine nucleotide exchange factor 7, Arhgef7	52725	0.0088
P04177	Tyrosine 3-monooxygenase, Th	492200	0.0819
P04937-2	Isoform 2 of Fibronectin, Fn1	259620	0.0432
P05197	Elongation factor 2, Eef2	807330	0.1344
P06238	Alpha-2-macroglobulin, A2m 2	5041300	0.8392
P06685	Sodium/potassium-transporting ATPase subunit alpha-1, Atp1a1	1911600	0.3182
P06761	78 kDa glucose-regulated protein, Hspa5	3669300	0.6108
P07153	Dolichyl-diphosphooligosaccharide--protein glycosyltransferase subunit 1, Rpn1 2	100390	0.0167
P07825	Synaptophysin, Syp	989900	0.1648
P10687	1-phosphatidylinositol 4, 5-bisphosphate phosphodiesterase beta-1, PLCβ1	334080	0.0556
P10719	ATP synthase subunit beta, mitochondrial, Atp5b	497690	0.0828
P11442	Clathrin heavy chain 1, Cltc	3468700	0.5774
P11507	Sarcoplasmic/endoplasmic reticulum calcium ATPase 2, Atp2a2	148630	0.0247
P11980-2	Isoform M2 of Pyruvate kinase PKM, Pkm	561270	0.0934
P12346	Serotransferrin, Tf	1157900	0.1927
P12785	Fatty acid synthase, Fasn	7,726.60	0.0013
P13383	Nucleolin, Ncl	1.24E+07	2.0562

P13635	Ceruloplasmin, Cp	641500	0.1068
P15865	Histone H1.4, Hist1h1e	3341300	0.5562
P15999	ATP synthase subunit alpha, mitochondrial, Atp5a1	1404700	0.2338
P16086	Spectrin alpha chain, non-erythrocytic 1, Sptan1	64746	0.0108
P16638	ATP-citrate synthase, Acly	298550	0.0497
P18292	Prothrombin, F2	366070	0.0609
P18395	Cold shock domain-containing protein E1, Csde1 2	74413	0.0124
P21575-2	Isoform 2 of Dynamin-1, Dnm1	182180	0.0303
P23514	Coatomer subunit beta, Copb1	149760	0.0249
P27008	Poly [ADP-ribose] polymerase 1, Parp1	301800	0.0502
P30427	Plectin, Plec	333190	0.0555
P32089	Tricarboxylate transport protein, mitochondrial, Slc25a1	841760	0.1401
P34058	Heat shock protein HSP 90-beta, Hsp90ab1	9610400	1.5998
P35427	60S ribosomal protein L13a, Rpl13a	300030	0.0499
P52873	Pyruvate carboxylase, mitochondrial, Pc	2126400	0.3540
P60711	Actin, cytoplasmic 1, Actb	7383900	1.2292
P62630	Elongation factor 1-alpha 1, Eef1a1 2	1.47E+07	2.4545
P62804	Histone H4, Hist1h4b	7417900	1.2348
P63018	Heat shock cognate 71 kDa protein, Hspa8	7621300	1.2687
P68035	Actin, alpha cardiac muscle 1, Actc1 2	4409600	0.7340
P68370	Tubulin alpha-1A chain, Tuba1a	1.65E+07	2.7482
P69897	Tubulin beta-5 chain, Tubb5	9725300	1.6189
P84245	Histone H3.3, H3f3b	1923400	0.3202
P85108	Tubulin beta-2A chain, Tubb2a	8447100	1.4061
P97536	Cullin-associated NEDD8-dissociated protein 1, Cand1	142200	0.0237
Q00438-2	Isoform PYBP1 of Polypyrimidine tract-binding protein 1, Ptbp1	692160	0.1152
Q01177	Plasminogen, Plg 2	1388700	0.2312
Q04462	Valine--tRNA ligase, Vars 2	293890	0.0489
Q04931	FACT complex subunit SSRP1, Ssrp1	204120	0.0340
Q05962	ADP/ATP translocase 1, Slc25a4	2.23E+07	3.7097
Q06000	Lipoprotein lipase, Lpl	1593000	0.2652
Q07647	Solute carrier family 2, facilitated glucose transporter member 3, Slc2a3	1180600	0.1965
Q09073	ADP/ATP translocase 2, Slc25a5	1.70E+07	2.8252
Q2PQA9	Kinesin-1 heavy chain, Kif5b	185300	0.0308
Q3KR86	MICOS complex subunit Mic60 (Fragment), Immt	466680	0.0777
Q3KR94	Protein Vtn, Vtn	1417400	0.2359
Q3KRE0	ATPase family AAA domain-containing protein 3, Atad3	168360	0.0280
Q4AEF8	Coatomer subunit gamma-1, Copg1 2	16241	0.0027

Q4G017	Nischarin, Nisch 2	333570	0.0555
Q4VSI4	Ubiquitin carboxyl-terminal hydrolase 7, Usp7	59660	0.0099
Q53UA7	Serine/threonine-protein kinase TAO3, Taok3	1622700	0.2701
Q5BJP4	Protein LOC100910882, Rbm39	446550	0.0743
Q5BK61	Sorting nexin-20, Snx20	2396500	0.3989
Q5FVC2	Rho guanine nucleotide exchange factor 2, Arhgef2	46967	0.0078
Q5M7T5	Protein Serpinc1, Serpinc1	1843800	0.3069
Q5M7V8	Thyroid hormone receptor-associated protein 3, Thrap3	236960	0.0394
Q5PPJ6	Leucyl-tRNA synthetase, Lars	341810	0.0569
Q5U2Y1-2	Isoform 2 of General transcription factor II-I, Gtf2i	70463	0.0117
Q5XHZ0	Heat shock protein 75 kDa, mitochondrial, Trap1	1802100	0.3000
Q5XI32	F-actin-capping protein subunit beta, Capzb	4210000	0.7008
Q5XI78	2-oxoglutarate dehydrogenase, mitochondrial, Ogdh	57888	0.0096
Q62780	Probable ATP-dependent RNA helicase DDX46, Ddx46	104040	0.0173
Q62910-2	Isoform 2 of Synaptojanin-1, Synj1	93171	0.0155
Q63041	Alpha-1-macroglobulin, A1m	3883900	0.6465
Q63357	Unconventional myosin-Id, Myo1d	98110	0.0163
Q63416	Inter-alpha-trypsin inhibitor heavy chain H3, Itih3 2	486020	0.0809
Q64268	Heparin cofactor 2, Serpind1	2182000	0.3632
Q66H86	Olfactomedin-like protein 1, Olfml1 2	2071200	0.3448
Q68FP1-2	Isoform 2 of Gelsolin, Gsn	4740500	0.7891
Q68FR6	Elongation factor 1-gamma, Eef1g 2	518930	0.0864
Q68G39	Cyclin-dependent kinase 16, Cdk16	1352500	0.2251
Q6AYI1	DEAD (Asp-Glu-Ala-Asp) box polypeptide 5, Ddx5	1357300	0.2259
Q6AYZ1	Tubulin alpha-1C chain, Tuba1c	1.55E+07	2.5774
Q6IFU9	Protein Krt16, Krt16	1711600	0.2849
Q6MG08	ATP-binding cassette sub-family F member 1, Abcf1	42505	0.0071
Q6MG90	Complement component 4, gene 2, C4b	1267500	0.2110
Q6P0K8	Junction plakoglobin, Jup	164620	0.0274
Q6P503	ATPase, H+ transporting, V1 subunit D, isoform CRA_c, Atp6v1d	2660900	0.4429
Q6Q0N3	5'-nucleotidase domain-containing protein 2, Nt5dc2 2	277730	0.0462
Q80ZA3	Alpha-2 antiplasmin, Serpinf1	980560	0.1632
Q8CG07	ATPase WRNIP1, Wrnip1	157120	0.0262
Q925G1-2	Isoform 2 of Hepatoma-derived growth factor-related protein 2, Hdgfrp2	56025	0.0093

Q9EPY0	Caspase recruitment domain-containing protein 9, Card9	83799	0.0139
Q9ESV6	Glyceraldehyde-3-phosphate dehydrogenase, testis-specific, Gapdhs	710190	0.1182
Q9JIL3-2	Isoform 2 of Interleukin enhancer-binding factor 3, Ilf3	781890	0.1302
Q9JJ31	Cullin-5, Cul5	110940	0.0185
Q9JKS6-2	Isoform 2 of Protein piccolo, Pclo	618890	0.1030
Q9QUL6	Vesicle-fusing ATPase, Nsf	56237	0.0094
Q9QYF3	Unconventional myosin-Va, Myo5a	757200	0.1260
Q9WUL0	DNA topoisomerase 1, Top1	62942	0.0105
Q9Z1P2	Alpha-actinin-1, Actn1	159790	0.0266
Q9Z1X1	Extended synaptotagmin-1, Esyt1	102530	0.0171
Q9Z327-2	Isoform 2 of Synaptopodin, Synpo	774410	0.1289

Table 1: Proteomics studies for PLCβ1 complexes.

Since stress granules are accumulation sites of stalled translation initiation complexes, we determined whether the level of PLCβ1 affected the ability of mRNA to be translated. This study was carried out by measuring protein synthesis in mock transfected PC12 cells or cells transfected with siRNA(PLCβ1) to obtain ~ 85-90% reduction in PLCβ1 levels. Protein synthesis was determined by measuring the amount of S^{35}-Methoinine/ Cysteine incorporated into the total amount of cellular protein. We find that in the PLCβ1 knock-down cells, the total protein levels increased nearly three times as compared to control suggesting that PLCβ1 has an inhibitory effect on protein synthesis (**Fig 2.1**). Together with the mass spectrometry data, these studies suggest

that PLCβ1 may be interacting with Ago2 and SG proteins, to reduce protein synthesis.

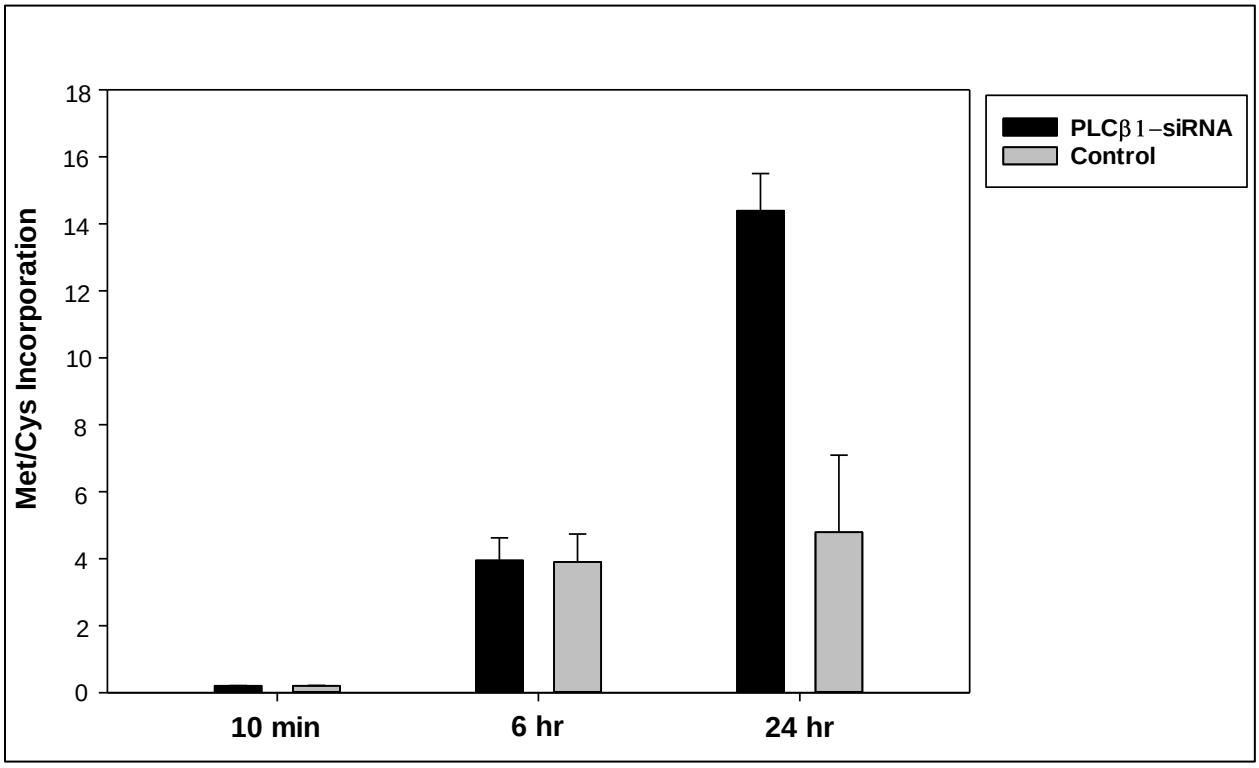

Figure 2.1: Protein synthesis measured by S^{35} methionine and cysteine incorporation where each value is normalized to total cell count for each measurement. In reduced PLCβ1 conditions protein synthesis is increased three times compared to control. Y axis scale $1*10^4$, Mean ±s.d. n= 2

PLCβ1 directly binds to Ago2. Our mass spectrometry data identified Ago2 as well as C3PO in PLCβ1 complexes, and in previous studies, we observed colocalization between PLCβ1 and Ago2 in HEK293 cells but only after treatment with siRNAs. These observations suggest that PLCβ1 and Ago2 proteins directly or indirectly associate but their interaction may be limited to certain cellular conditions, such as stress. Therefore, we carried out studies to better characterize PLCβ1 / Ago2 interactions in cells. We first carried out mass spectrometry studies in which we

identified proteins associated with Ago2. We found that PLCβ1 is a major component in Ago2 complexes. We then visualized their interactions in PC12 cells by transfecting fluorescent-tagged PLCβ1 and Ago2 and assessing their interaction by Förster resonance energy transfer (FRET). In these measurements FRET was determined by the reduction in the fluorescence lifetime of the donor (i.e. eGFP-PLCβ1) when it is in the presence of a FRET acceptor (mCherry-Ago2). By measuring the lifetime of the eGFP in each pixel of an image of a cell expressing eGFP-PLCβ1, and its reduction when mCherry-Ago2 is present, we can determine the cellular location of eGFP-PLCβ1 and eGFP-PLCβ1 / mCherry-Ago2 complexes, and how the distribution changes under stress. In **Fig. 2.2** we show FLIM (fluorescence lifetime imaging micrographs) of undifferentiated PC12 cells expressing eGFP-PLCβ1. This image shows that the enzyme localizes to the plasma membrane and cytosol but not to the nucleus.

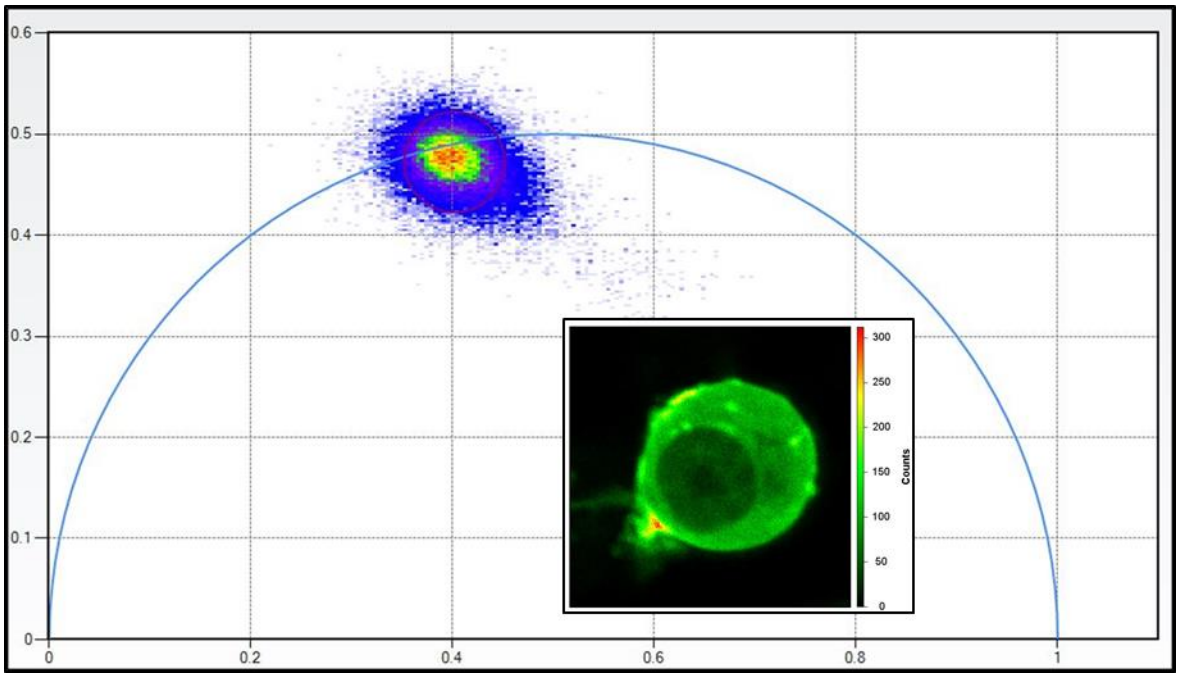

Figure 2.2: PC12 cells expressing eGFP-PLCβ1 alone. eGFP-PLCβ1 alone shows a uniform species centered on the arc of FLIM Phasor plot. Hotter colors in cell images correspond to higher intensity and in the phasor plot correspond to number of pixels.

When the cells are co-transfected with mCherry-Ago2, we find a reduction in the lifetimes of the cytosolic populations. To determine whether the proteins were associated, we assessed the amount of FRET by the reduction in lifetime and plotted the data on a phasor diagram. In these diagrams the lifetime of each pixel is plotted in a form that allows one to directly assess whether the lifetime is from a single population, and on the phasor arc, or from a mixed population which is seen inside the phasor. If eGFP-PLCβ1 is within ~20A from the mCherry-Ago2, its net lifetime will decrease due to FRET causing the points to move into the phasor arc. This behavior is seen in **Fig. 2.3.**

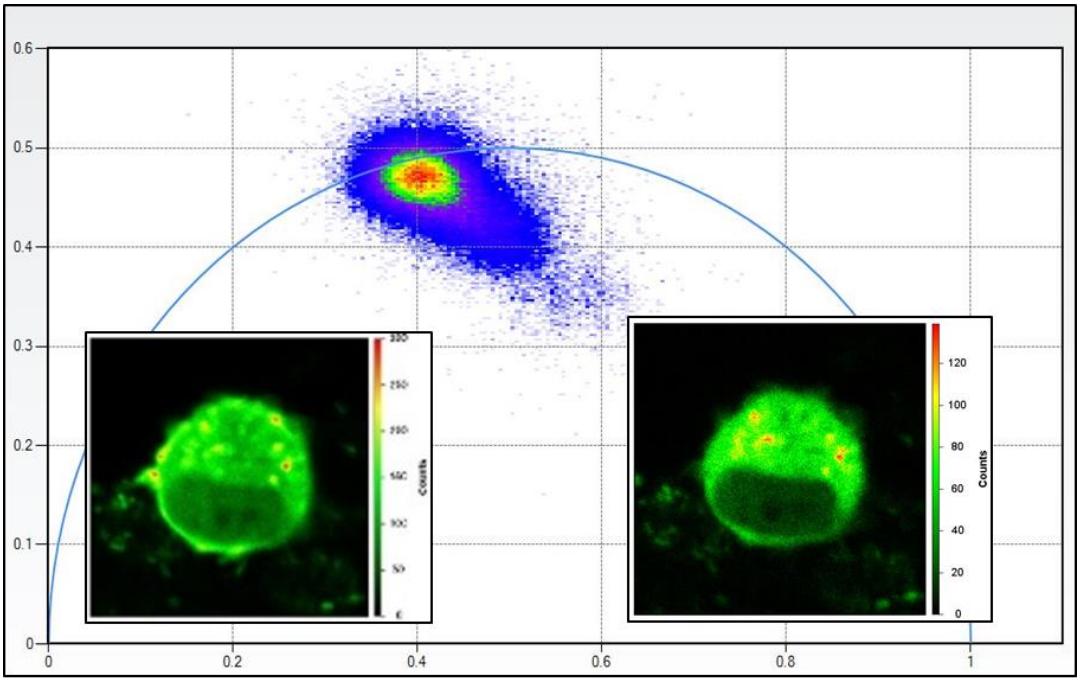

a b

Figure 2.3: PC12 cells expressing eGFP-PLCβ1 and mCherry-Ago2. Association shown by decrease in eGFP lifetime as it transfers its energy to mCherry via FRET. In the presence of mCherry-Ago2 (b), the lifetimes of eGFP-PLCβ1 (a) move inside the arc towards shorter lifetimes.

Hotter colors in cell images correspond to higher intensity and in the phasor plot correspond to number of pixels.

The advantage of using a phasor representation as opposed to the normal lifetime decay curves (i.e. the Fourier transform of the phasor), is that reduction in lifetime are assessed from the raw data without the need for model-dependent fitting or correction of background. Association between the two proteins is clearly seen in **Fig. 2.4.**

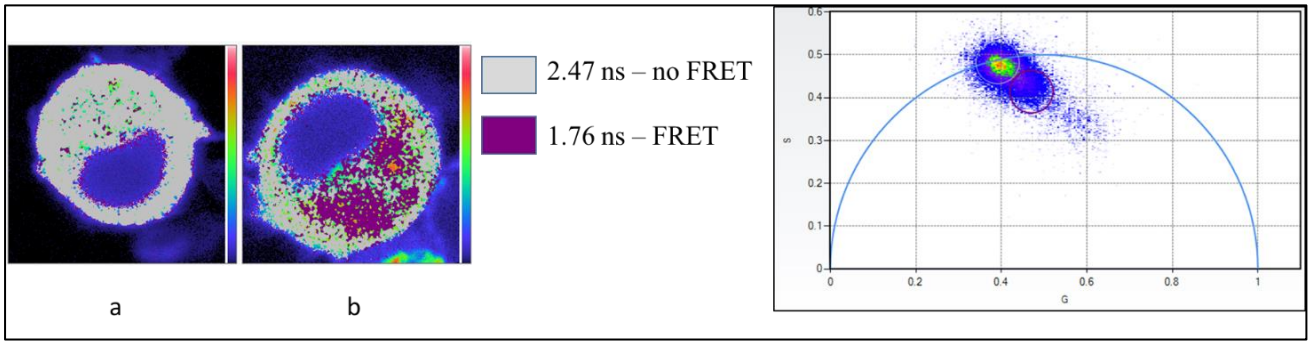

Figure 2.4: FLIM phasor plot showing FRET between eGFP-PLCβ1 and mCherry-Ago2 in PC12 cells in cytosolic regions. a- shows cell expressing eGFP-PLCβ1, b- shows cell expressing eGFP-PLCβ1 and mCherry-Ago2. Grey regions have higher lifetime compared to purple region.

PLCβ1 moves into cytoplasm when the cells experience osmotic stress. We wanted to determine the cellular signals that contribute to the association between PLCβ1, Ago2 and other stress granule proteins. We had previously found that a portion of the plasma membrane population of PLCβ1 changes its localization under stress conditions. We directly tested this idea by monitoring changes in localization of endogenous PLCβ1 in PC12 cells subjected to mild hypo-osmotic stress (300 to 150 mOsm). We find that a significant portion of the plasma membrane population shifts to the cytosol as shown in **Fig. 2.5**. We further quantified this relocalization by

looking at changes in the endogenous PLCβ1 distribution when subjected to osmotic stress. For this experiment, we immunostained the cells for PLCβ1 before and after 30 minutes of stress and viewed the distribution using a confocal fluorescence microscope. We then compared the cytosolic intensity before and after applying the stress and find that cytosolic PLCβ1 levels are significantly higher when the cell is subjected to osmotic stress.

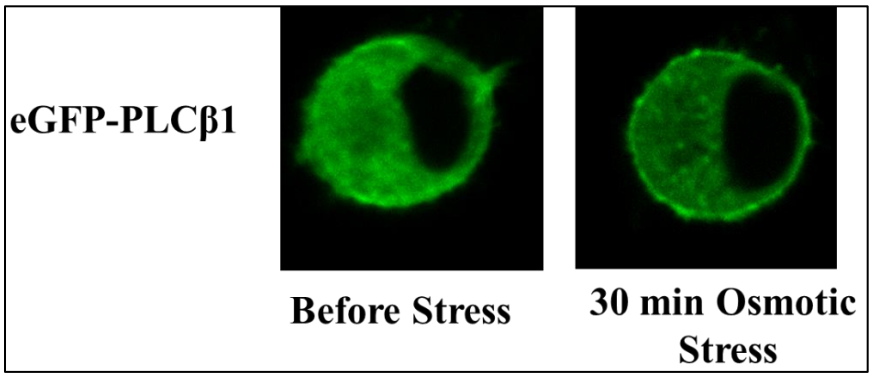

Figure 2.5. PC12 cells expressing eGFP-PLCβ1 subjected to 30 min of osmotic stress.

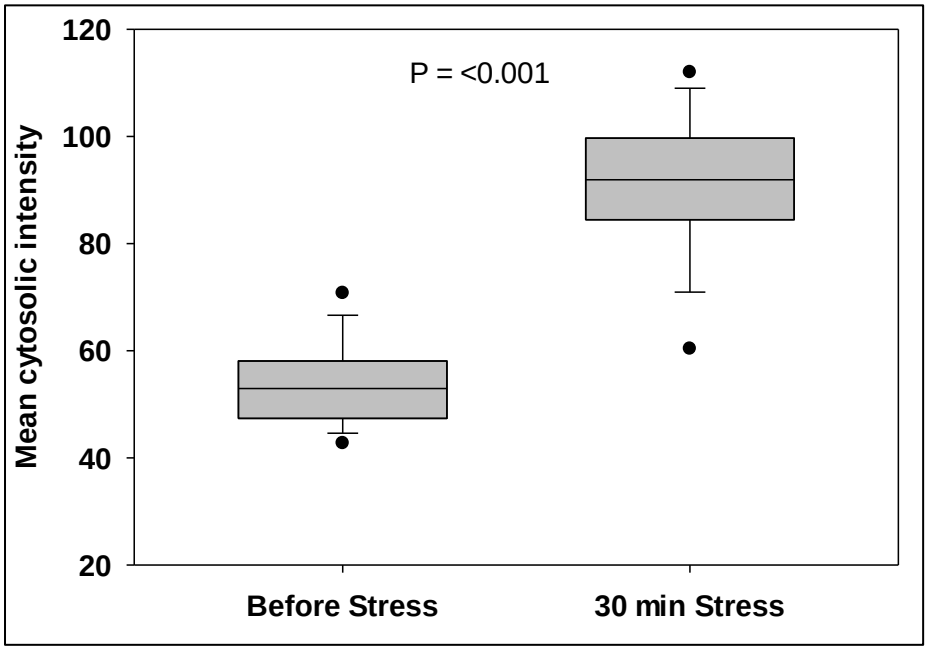

Figure 2.6: Comparison of cytosolic levels of PLCβ1 between normal PC12 cells and cells subjected to 30 minutes of osmotic stress. PC 12 cells were immunostained for PLCβ1 under conditions of osmotic stress. N>40 cells for each condition. Optical slice thickness< 0.8 um

We reasoned that this movement of PLCβ1 into the cytosol would reduce its ability to transduce calcium signals from an extracellular stimulus. Using a fluorescent calcium indicator, we measured the response of PC12 cells stimulated with acetylcholine to activate the Gαq/PLCβ pathway. We find that when cells are subjected to hypo-osmotic stress, calcium signals are lowered, presumably due to a reduced population of PLCβ at the plasma membrane (**Fig. 2.7**).

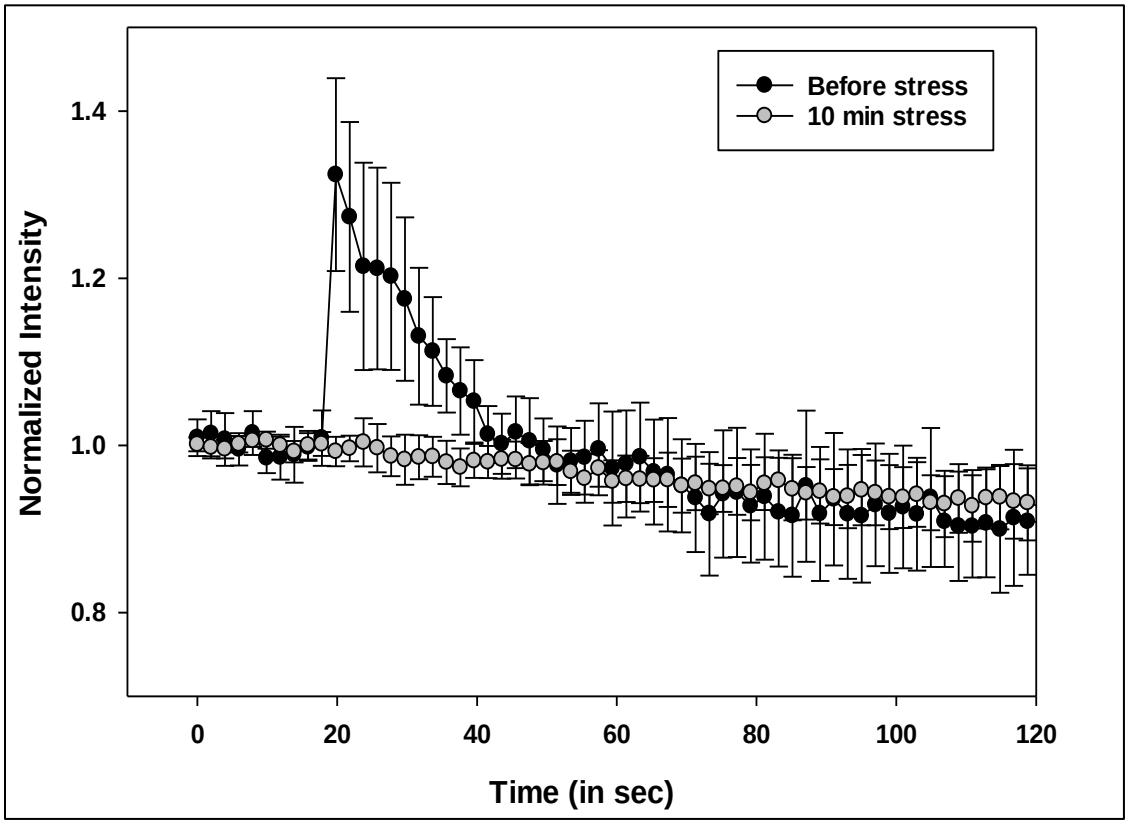

Figure 2.7: Hypo-osmotic stress reduces PLCβ1-mediated Ca2+ signals in cultured PC12 cells.

Cultured PC12 cells on 35 mm glass bottom dishes were incubated with Fura-2-AM. Change in fluorescence was monitored before and after stimulation with 5uM carbachol at 18 s. Black circles, cells before stress; gray circles, cells under stress for 10 min. Fluorescence intensity levels normalized to basal levels before stimulation for each cell. n = 12; Mean + s.d. is shown. ***This study shows that inclusion of PLCβ1 in SGs ablates its ability to mediate calcium responses.***

We then determined whether the hypo-osmotic stress that causes movement of PLCβ1 into the cytosol results in increased interaction with Ago2. In these experiments, we measured changes in the association between eGFP-PLCβ1 and mCherry-Ago2 when subjected to hypo-osmotic stress by the reduction in lifetime of GFP-PLCβ1 to indicate FRET. FLIM imaging, showed that the membrane fraction of PLCβ1 has a higher lifetime that can be distinguished from the shorter lifetime population in the cytosol associated with Ago2 (**Fig. 2.8)**. When osmotic stress was applied, the longer lived population on the membrane is reduced while the shorter lived population in the cytosol is increased. This result is consistent with PLCβ1 dissociating from Gαq on the plasma membrane to bind to Ago2 and other cytosolic, stress granule proteins.

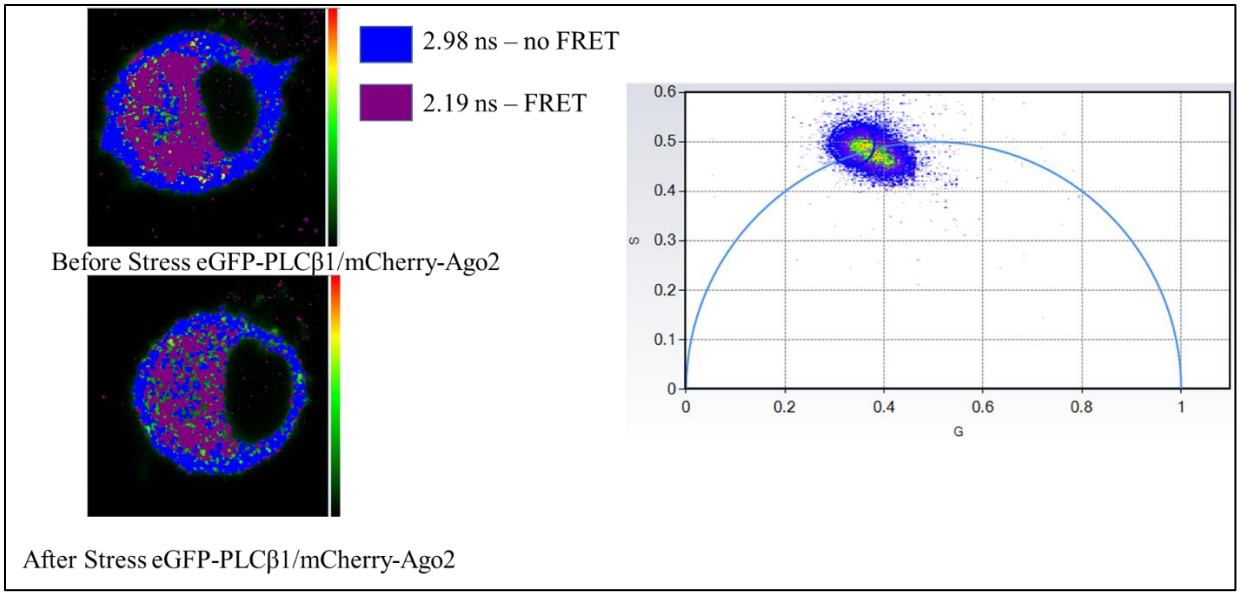

Figure 2.8: FLIM phasor plot to characterize association between PLCβ1-Ago2 under osmotic stress conditions for PC12 cells co-expressing eGFP-PLCβ1and mCherry-Ago2

PLCβ1 interacts with Ago2 in stress granules during osmotic stress. Since PLCβ1 binds to translation initiation proteins and stress granule proteins, we hypothesized that it moves to stress granules to inhibit protein translation in response to osmotic stress. Polyadenylate binding protein C1 (PABPC1) is associated with the formation of stress granules and is often used as stress granule marker [26]. Thus, we monitored changes in the co-localization of PLCβ1 and PABPC1 before, during and after hypo-osmotic stress. Before stress, we find a basal level of co-localization which correlates with our mass spectrometry data. Upon dilution of the media to reduce the osmolarity, we find a significant increase in co-localization that recovers once the osmolarity is returned to basal levels as shown in **Fig. 2.9**.

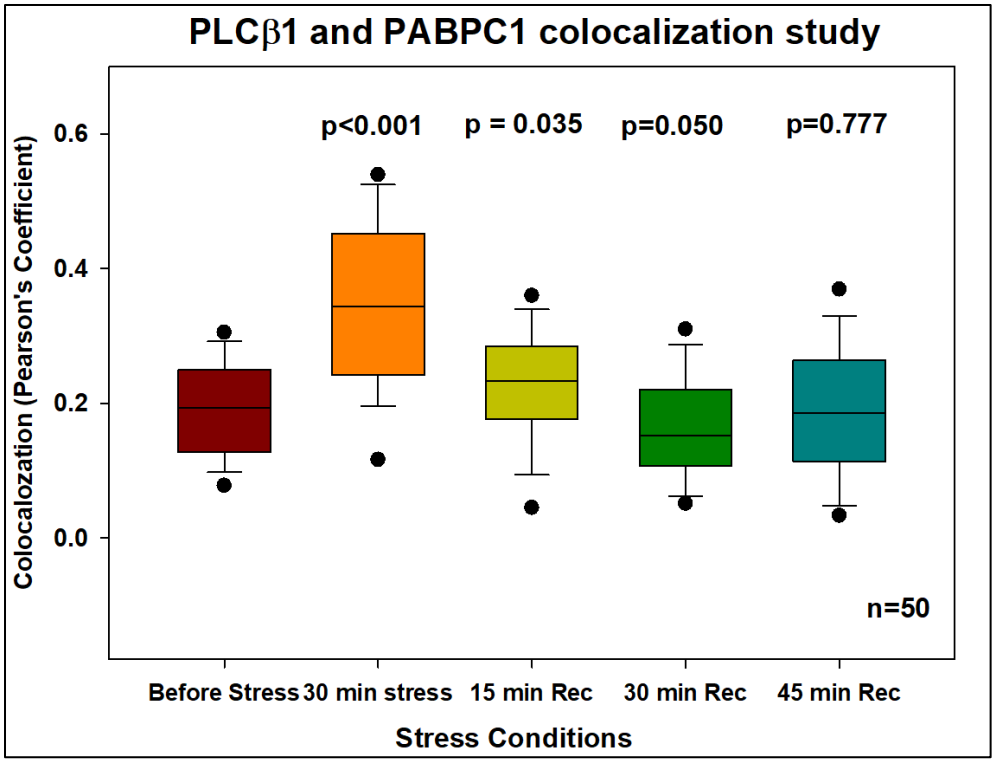

Figure 2.9: Co-localization of PLCβ1 and PABPC1 before, during and after hypo-osmotic stress in PC12 cells. N=50 cells. p values are in comparison to before stress control.

We also followed the association between PLCβ1-Ago2 under osmotic stress conditions. Changes in the lifetime of GFP-PLCβ1 alone or with mCherry-Ago2 in PC12 cells were followed using FRET/FLIM. We isolated the population of PLCβ1 that binds Ago2 by monitoring the appearance of a shift in lifetimes towards short lived molecules that participate in FRET with mCherry-Ago2. We find the dynamics of these populations change when subjected to stress. When stress is applied, PLCβ1 remains constitutively bound to Ago2 and the long lived membrane population of PLCβ1 moves into the cytoplasm which results in increased binding to Ago2. (see **Fig. 2.10**). However, when the stress is removed, the lifetime distribution shifts towards the short lived population. Together with the FLIM/FRET studies, these results show increased association

between PLCβ1 and Ago2 with stress. We interpret these results as movement of the proteins into a region, such as a stress granule, where the fluorophores are held in a conformation where partial FRET occurs. Releasing the stress results in a tighter binding between PLCβ1 and Ago2 probably to help cells survive post stress.

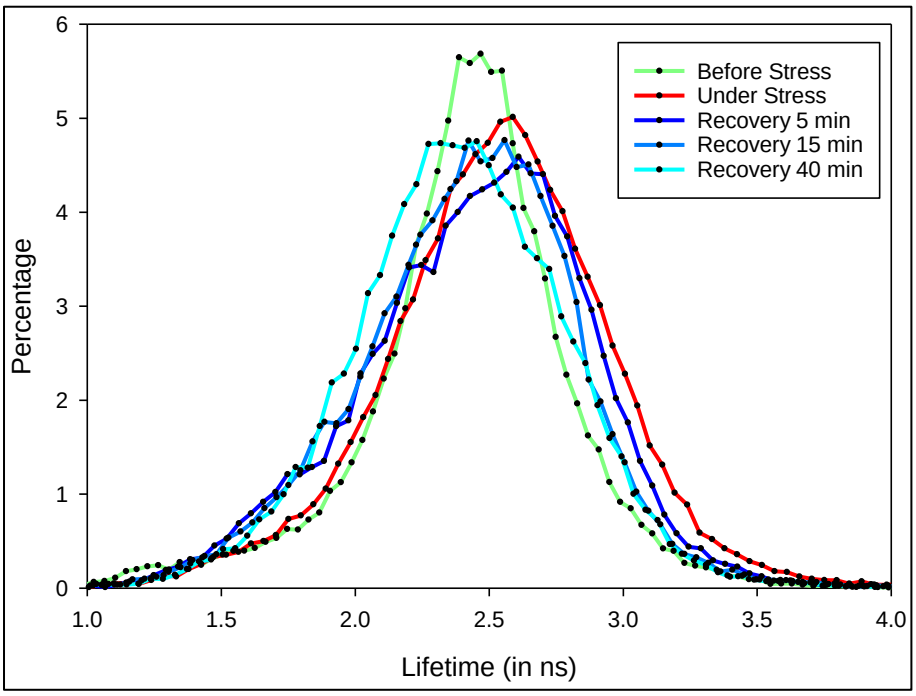

Figure 2.10: PLCβ1-Ago2 FLIM during and after Osmotic Stress in PC12 cells

We tested this idea by monitoring the diffusion of eGFP-PLCβ1 and find that the change in mobility before, during and after release of stress is consistent with PLCβ1 moving into the cytosol to bind Ago2 and stress proteins when hypo-osmotic conditions are introduced. Upon release, PLCβ1 then dissociates to more freely in the cytosol and bind to its cytosolic partners (**Fig. 2.11**).

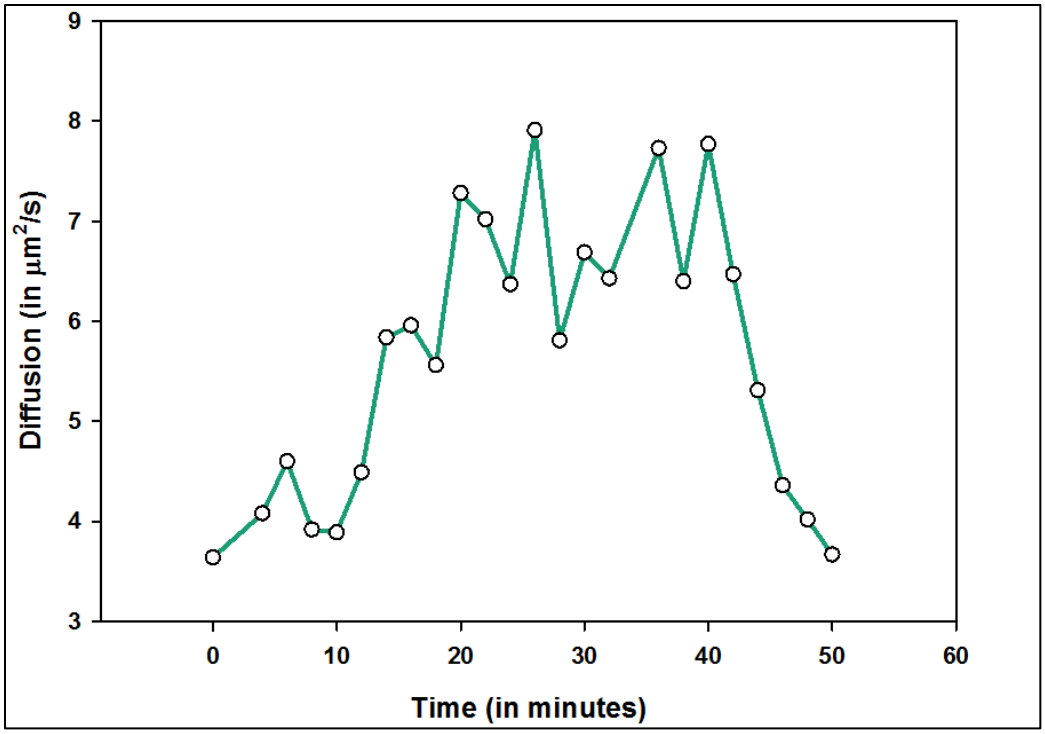

Figure 2.11: Diffusion of YFP-PLCβ1 during and after hypo-osmotic stress in PC12 cells using FCS spectroscopy. Recovery starts after 30 minutes.

Movement of PLCβ with osmotic stress occurs in smooth muscle cells. Unlike PC12, smooth muscles cells are functionally adapted to tolerate changes in osmotic stress. We tested whether similar changes in PLCβ movement occur in cultured rat aortic smooth muscle cells (A10). The Scarlata group had previously found that osmotic stress results in deformation of caveolae domains in the plasma membrane which eliminates interactions between caveolins and Gαq (reference). Because these cells are thin, it is difficult to image changes in PLCβ1 localization from the plasma membrane to the cytosol. Therefore, we assessed re-localization by increased co-immunoprecipitation with Ago2 (**Fig. 2.12**), and we monitored an increase in PLCβ1 association

with the cytosolic protein C3PO as compared to controls (**Fig. 2.13**). Together, these results suggest movement of PLCβ1 into the cytosol to bind Ago2 upon osmotic stress.

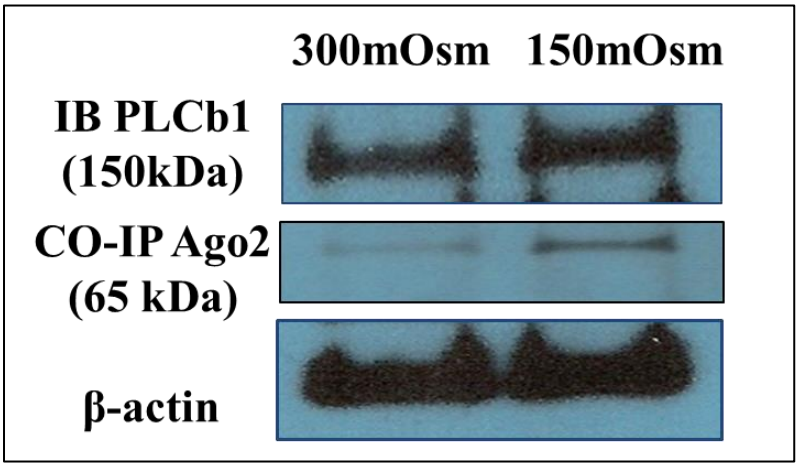

Figure 2.12: Western blot showing increased co-immunoprecipitation of Ago2 with PLCβ1 when subjected to osmotic stress in A10 cells

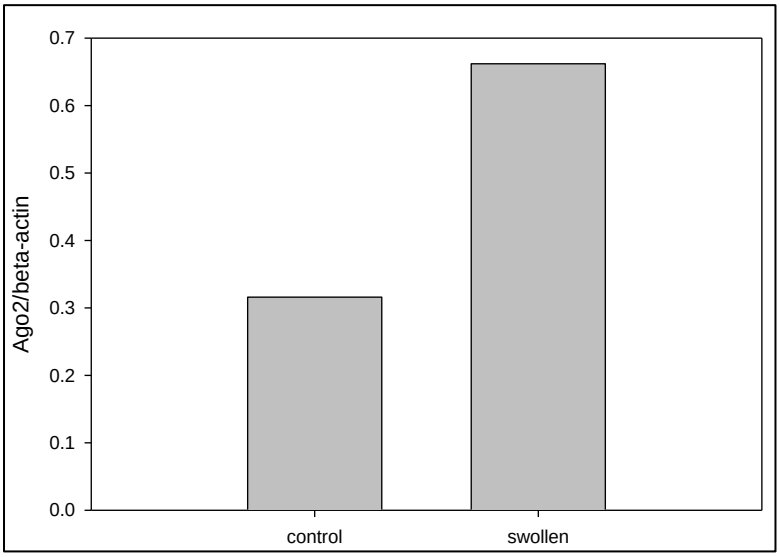

Figure 2.13: Increased association of PLCβ1 with the cytosolic protein C3PO as compared to controls

PLCβ1 levels and osmotic stress impact the let7 family of miR We determined the impact of PLCβ1 levels on the miR populations in undifferentiated PC12 cells, and then tested whether similar changes occur in A10 cells undergoing osmotic stress. In the first series of experiments, we extracted miRNAs from PC12 cells transfected with control siRNA or with siRNA (PLCβ1) for 24 hours and performed RNA sequencing. While the expression of several miRs were perturbed as a result of knocking down PLCβ1, we find that PLCβ1 expression had the highest impact on members of the *let7* family of miRNAs (**Table 2**).

miRNA ID	PLCβ1 control	PLCβ1 KO	Fold difference
rno-let-7i-5p	128640	84470	1.52
rno-let-7f-5p	83682	52824	1.58
rno-let-7f-5p	82726	51871	1.59
rno-let-7g-5p	74580	50190	1.48
rno-let-7a-5p	28115	18426	1.52
rno-let-7a-5p	28105	18434	1.52
rno-let-7c-5p	27824	18525	1.50
rno-let-7c-5p	27661	18433	1.50
rno-let-7d-5p	19450	11824	1.64
rno-let-7b-5p	13177	8818	1.49
rno-let-7e-5p	7883	5306	1.48
rno-let-7d-3p	1856	1146	1.61
rno-let-7a-1-3p	1537	1016	1.51
rno-let-7c-2-3p	1536	1016	1.51
rno-let-7i-3p	397	239	1.66

Table 2: miRNA changes due to change in PLCβ1 expression in PC12 cells

We then carried out a similar study in which we compared the miR population of A10 cells under basal conditions and 5 minutes after begin subjected to hypo-osmotic stress. Overall, the miR populations showed only minor changes except for members of the *let7* family (i.e. *let7a-7h*) (see **Table 3**). Thus, diminishing the cellular level of PLCβ1, or sequestering it into stress granules produces similar effects on a major miR family, *let7*.

miRNA ID	Swollen	Control	Fold difference
rno-let-7i-5p	5155.00	6381.67	0.81
rno-let-7f-5p	4495.33	5454.67	0.82
rno-let-7f-5p	4454.33	5399.67	0.82
rno-let-7c-5p	1997.67	2430.67	0.82
rno-let-7c-5p	1844.00	2198.67	0.84
rno-let-7b-5p	1497.00	1606.33	0.93
rno-let-7g-5p	1107.67	1829.00	0.61
rno-let-7a-5p	892.00	1177.67	0.76
rno-let-7a-5p	840.00	1121.67	0.75
rno-let-7e-5p	416.67	523.33	0.80

Table 3: miRNA changes upon subjecting the cells to osmotic stress in A10 cells

Let7 impacts a host of regulatory pathways and responds to alternations in cell environment. Aside from regulating oncogenes, such as *myc* and in turn growth pathways, *let7* impacts growth and proliferation pathways that culminate in glucose levels [19]. We measured the changes in glucose levels of A10 cells subjected to mild osmotic stress. We find a large and systematic loss in cellular glucose over time that may correlative to changes in let7 levels (**Fig. 2.14**).

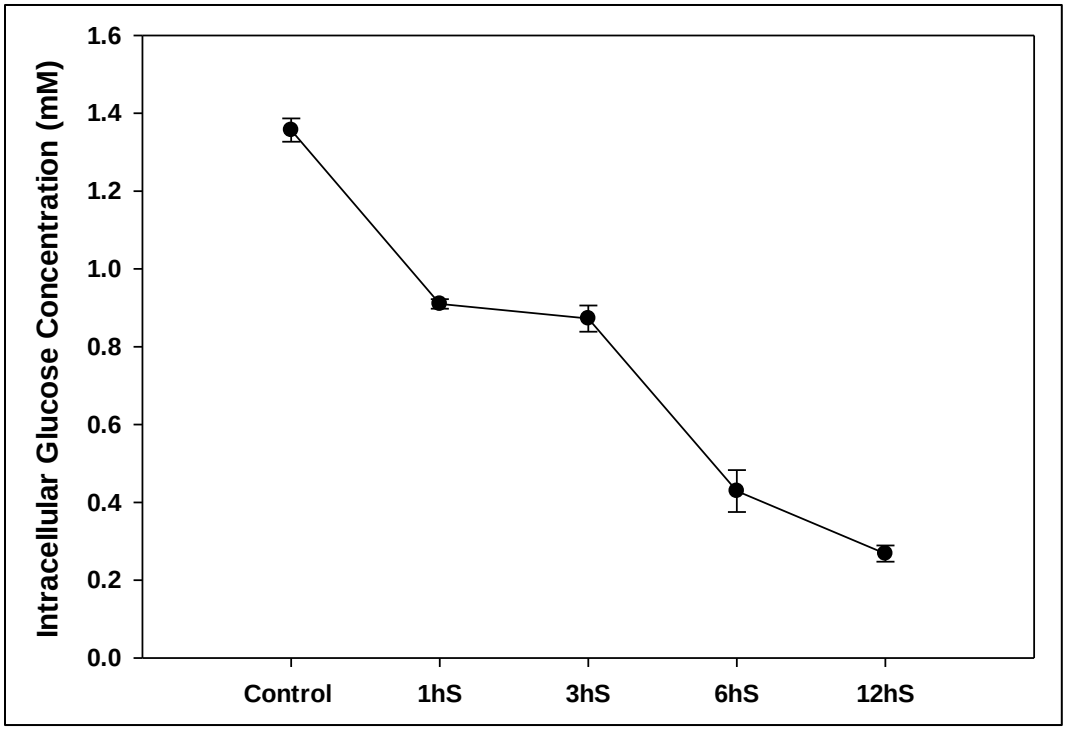

Figure 2.14: Decrease in glucose levels in A10 smooth muscle cells subjected to mild osmotic stress

DISCUSSION

Stress granules are non-membrane organelles that sequester mRNA and proteins associated with the transcriptional machinery. Stress granules act as storage centers that allow cells to decide whether to transcribe, continue to store or degrade mRNA [12-15]. While stress granules are present under basal conditions, many form when cells experience rapid changes in cell environment and in 'emergency' situations. The ability of cells to organize and dissolve stress granules is thought to underlie a variety of human diseases but the mechanism(s) that relays changes in the external environment that promote the formation of stress granules is unknown. In

this study, we have found that PLCβ can act as a sensor that monitors external information signal when stress granules should form.

PLCβ has been known to play a key role in mediating extracellular sensory information received by the Gq family of heterotrimeric G proteins (i.e. hormones and neurotransmitters) to generate calcium signals that lead to proliferative and mitogenic changes in cells [1-3]. Although PLCβ binds to membranes to access its main substrate, PIP2, PLCβ is highly soluble. Under most conditions, we find that a substantial population resides on the plasma membrane where it associates with Gq. Several years ago our lab discovered that PLCβ can move from the plasma membrane to the cytoplasm to bind to a complex that has been reported to promote RNA-induced silencing [23]. Specifically, C3PO (component 2 of RISC) is thought to digest the passenger strand of silencing RNAs after an initial nick by Ago2, which is the main nuclease component of the RNA-induced silencing complex (RISC). While C3PO binding has no effect on PLCβ activity, PLCβ inhibits the ability of C3PO to hydrolyze specific RNA sequences [25].

In our previous studies, we observed evidence that PLCβ may also associate to Ago2 which prompted us to study this association. Using mass spectrometry to analyze the proteins in PLCβ complexes, we found that Ago2 is present in PLCβ complexes and we verified their direct binding in cells by FLIM/FRET. However, we could not detect association between C3PO and Ago2. This result shows that C3PO promotes RISC by a mechanism that does not involve direct association. The lack of interaction between Ago2 and C3PO lead us to believe that PLCβ binding to Ago2 might serve another function besides inhibiting RNA-induced silencing. Turning again to our mass spectrometry data, we find that roughly a third of the protein mass associated with PLCβ consists of 3 stress granule proteins including one (PABPC1) that is exclusively found in stress granules (Table 1).

Stress granules must form rapidly under adverse conditions and it is not surprising that cells have adapted a feedback mechanism to promote stress granule formation under appropriate environmental conditions [12]. Our data show that PLCβ acts as a sensor to help orchestrate part of the stress response. Specifically, we find that in response to osmotic stress, PLCβ1 moves from the plasma membrane to the cytoplasm where it interacts with Ago2 into stress granules. This process has the net effect of reducing G protein responses to sensory information while protecting mRNA from degradation. Upon release of stress, PLCβ appears to move out of the stress granules and have increased binding with Ago2.

Our results show a large change in the level of members of *let* family of miRs when PLCβ1 and Ago2 incorporate into stress granule. *Let* miRs, from *lethal* in drosophila, are responsible for metabolic responses to stress [19]. *Let* miRs are thought to be constitutively bound to Ago2 regulate the expression of metabolic enzymes. By sequestering Ago2 into stress granules, these mRNA are preserved and ready to be transcribed when the stress is removed. The observation that when stress is removed, PLCβ has increased interaction with Ago2 suggests that PLCβ helps Ago2 to restore its normal function by regulating gene expression.

METHODS

Cell culture: PC12 cells were cultured in high glucose DMEM (GIBCO) with 10% heat-inactivated horse serum (GIBCO) and 5% fetal bovine serum (Atlanta Biologicals). HEK293 and A10 cell lines were cultured in high glucose DMEM with 10 % fetal bovine serum. All cells were incubated at 37°C in 5% CO_2.

Plasmids: EGFP-hAgo2 was a gift from Phil Sharp (Addgene plasmid # 21981). MCherry-Ago2 was a gift from Alissa Weaver (Vanderbilt University). MCherry-TRAX-C1 plasmid was constructed by inserting TRAX gene between BamHI and EcoRI restriction sites in mCherry-C1 backbone using T4 DNA ligase (NEB). Plasmid transfections and siRNA knock-downs were done using Lipofectamine 3000 (Invitrogen) in antibiotic-free media. Media was changed to one containing antibiotic (1% Penicillin/Streptomycin) 6 hours post-transfection. For every FLIM experiment, two separate samples were prepared: donor alone, donor in presence of acceptor.

Co-immunoprecipitation: PC12 cells were lysed in buffer containing 1% Triton X-100, 0.1% SDS, 1x protease inhibitor cocktail and 10 mM Tris, pH 7.4. 200 μg of soluble protein was incubated with 2 μl of PLCβ1/Ago2 antibody overnight at 4 °C. After addition of 20 mg of protein A-Sepharose 4B beads (Invitrogen), the mixture was gently rotated for 4 h at 4 °C. Beads were washed three times with lysis buffer, and bound proteins were eluted with sample buffer for 5 min at 95 °C. Precipitated proteins were loaded onto two 10% polyacrylamide gel. After SDS-PAGE one gel was transferred to polyvinylidene difluoride membranes, proteins were detected by immunoblotting with anti-PLCβ1 (D-8, Santa Cruz) and anti-Ago2 (Abcam) antibody. For the other gel was used for Mass spectrometry.

Sample Preparation for Mass Spectrometry: Short gel bands were cut and sent to UMass Medical School Mass spec facility. The results obtained were opened in Scaffold Viewer and the identified proteins were categorized using DAVID analysis.

Osmotic Stress Experiments: For all the osmotic stress experiments, the cells were subjected to 10-30 min of stress by diluting the media with 50% water.

Immunoflourescence Experiments: PC 12 cells were washed 2x with PBS to remove dead cells. Then were fixed with 3.7% paraformaldehyde in PBS for 10 min. They were further permeabilized 3x using MSM pipes buffer (0.1% Trition-X 100 in PBS) for 7-10 minutes. Blocking was done for 30 minutes using 4% goat serum, 1% BSA and 50mM glycine. Cells were further incubated with primary antibody (1:500 in 1%BSA solution in PBS) overnight and next day washed 3x using 1%BSA solution in PBS. Then the cells were incubated with their respective secondary antibodies for 45 min and then washed 3x PBS. Cells were transferred in PBS for viewing using LSM 510 Zeiss Confocal Microscope.

FCS—FCS measurements were performed on a dual-channel confocal fluorescence correlation spectrometer (Alba version 5, ISS Inc.) equipped with avalanche photodiodes and a Nikon Eclipse Ti-U inverted microscope. A x60 Plan Apo (1.2 NA, water immersion) objective and a mode-locked two-photon titanium-sapphire laser (Tsunami; Spectra-Physics) was used in this study. The waist (ω0) of the excitation beam was calibrated each time before experiments by measuring the diffusion of Alexa Fluor 488 in water with a diffusion coefficient of 435 μm^2 /s (Ref). The typical ω0 values were 0.43– 0.45 µm. Cells expressing low amounts of YFP-PLCβ protein were selected for viewing. The samples were excited at 940 nm, and emission spectra were collected through a 542/27 bandpass filter. The data were acquired in the time mode for 120 s, and the sampling frequency was 100 kHz. Measurements that showed abrupt and significant changes in the count rate were neglected to avoid artifacts due to bleaching and/or cell movement. The data were stored and processed by Vista software (ISS Inc.). The autocorrelation functions were analyzed using a, one-component three-dimensional Gaussian diffusion model provided by ISS software.

FLIM—FLIM measurements were performed on the dual-channel confocal fast FLIM(Alba version 5, ISS Inc.) equipped with photomultipliers and a Nikon Eclipse Ti-U inverted microscope.

A x60 Plan Apo (1.2 NA, water immersion) objective and a mode-locked two-photon titanium-sapphire laser (Tsunami; Spectra-Physics) was used in this study. The lifetime of the laser was calibrated each time before experiments by measuring the lifetime of Atto 435 in water with a lifetime of 3.61 ns (Ref) at 80MHz, 160MHz and 240MHz. The samples were excited at 800/850 nm, and emission spectra were collected through a 525/50 bandpass filter. For each measurement, the data was acquired until the photon count was greater than 300. The data were stored and processed by Phasor fitting analysis. For osmotic stress experiments, the phasor plot data containing S and G values was exported and the lifetime was calculated using the equation

$$t = \frac{S}{G * 2\pi * \omega}$$

For calculating lifetime ω used was 80 MHz

Statistical analysis: Data was analyzed using Sigma Plot 13 statistical packages that included student's t-test and one way analysis of variance (ANOVA).

BIBLIOGRAPHY

1. Suh, P.G., et al., *Multiple roles of phosphoinositide-specific phospholipase C isozymes.* BMB Rep, 2008. **41**(6): p. 415-34.
2. Rebecchi, M.J. and S.N. Pentyala, *Structure, function, and control of phosphoinositidespecific phospholipase C.* Physiol Rev, 2000. **80**(4): p. 1291-335.

3. Rhee, S.G., *Regulation of phosphoinositide-specific phospholipase C.* Annu Rev Biochem, 2001. **70**: p. 281-312.

4. Jiang, H., et al., *Roles of phospholipase C beta2 in chemoattractant-elicited responses.* Proc Natl Acad Sci U S A, 1997. **94**(15): p. 7971-5.

5. Urena, J., A. del Valle-Rodriguez, and J. Lopez-Barneo, *Metabotropic Ca2+ channelinduced calcium release in vascular smooth muscle.* Cell Calcium, 2007. **42**(4-5): p. 51320.

6. Essen, L.O., et al., *Crystal structure of a mammalian phosphoinositide-specific phospholipase C delta.* Nature, 1996. **380**(6575): p. 595-602.

7. Paterson, H.F., et al., *Phospholipase C delta 1 requires a pleckstrin homology domain for interaction with the plasma membrane.* Biochem J, 1995. **312 (Pt 3)**: p. 661-6.

8. Lyon, A.M., et al., *Full-length Galpha(q)-phospholipase C-beta3 structure reveals interfaces of the C-terminal coiled-coil domain.* Nat Struct Mol Biol, 2013. **20**(3): p. 35562.

9. Drin, G. and S. Scarlata, *Stimulation of phospholipase Cbeta by membrane interactions, interdomain movement, and G protein binding--how many ways can you activate an enzyme?* Cell Signal, 2007. **19**(7): p. 1383-92.

10. Taylor, S.J., et al., *Activation of the beta 1 isozyme of phospholipase C by alpha subunits of the Gq class of G proteins.* Nature, 1991. **350**(6318): p. 516-8.

11. Protter, David S.W. et al., *Principles and Properties of Stress Granules*. Trends in Cell Biology 2016, Volume 26 , Issue 9 , 668 – 679

12. Buchan, J. Ross, and Roy Parker., *Eukaryotic Stress Granules: The Ins and Out of Translation*. Molecular cell, 2009. 36.6: 932

13. Decker, C. J., & Parker, R., *P-Bodies and Stress Granules: Possible Roles in the Control of Translation and mRNA Degradation*. Cold Spring Harbor Perspectives in Biology 2012, 4(9), a012286.

14. Anderson, Paul, and Nancy Kedersha. *RNA Granules*.The Journal of Cell Biology 2006,172.6: 803–808

15. Leung AKL, Calabrese JM, Sharp PA. *Quantitative analysis of Argonaute protein reveals microRNA-dependent localization to stress granules*. Proceedings of the National Academy of Sciences of the United States of America. 2006;103(48):18125-18130. doi:10.1073/pnas.0608845103.

16. Hammond Scott M., *Dicing and slicing*, FEBS Letters 2005, 579

17. Karginov FV, Hannon GJ. *Remodeling of Ago2–mRNA interactions upon cellular stress reflects miRNA complementarity and correlates with altered translation rates*. Genes & Development. 2013;27(14):1624-1632

18. Hartig SM, Hamilton MP, Bader DA, McGuire SE. *The microRNA interactome in metabolic homeostasis.* Trends in endocrinology and metabolism: TEM. 2015;26(12):733-745.

19. Zhu H, Shyh-Chang N, Segrè AV, et al. *The Lin28/let-7 axis regulates glucose metabolism*. Cell. 2011;147(1):81-94. doi:10.1016/j.cell.2011.08.033.

20. Sahu, S., F. Philip, and S. Scarlata, *Hydrolysis rates of different small interfering RNAs (siRNAs) by the RNA silencing promoter complex, C3PO, determines their regulation by phospholipase Cbeta*. J Biol Chem, 2014. **289**(8): p. 5134-44.

21. Hüttelmaier, S., et al., *Spatial regulation of β-actin translation by Src-dependent phosphorylation of ZBP1*. Nature, 2005. 438: p. 512.

22. Shovon I. Ashraf et al, Synaptic *Protein Synthesis Associated with Memory Is Regulated by the RISC Pathway in Drosophila*, Cell, 2006. **124**(1), p.191-205

23. Garwain O., ,Scarlata S. *Phospholipase Cβ-TRAX Association Is Required for PC12 Cell Differentiation*. Journal of Biological Chemistry 2016,291(44):22970-22976.

24. Aisiku OR, Runnels LW, & Scarlata S. *Identification of a Novel Binding Partner of Phospholipase Cβ1: Translin-Associated Factor X*. PLoS ONE 2010, 5(11):e15001.

25. Philip F, Sahu S, Golebiewska U, & Scarlata S *RNA-induced silencing attenuates G protein-mediated calcium signals.* FASEB 2016,30(5):1958-1967.

26. Burgess, Hannah M. et al. *Nuclear Relocalisation of Cytoplasmic poly(A)-Binding Proteins PABP1 and PABP4 in Response to UV Irradiation Reveals mRNA-Dependent Export of Metazoan PABPs.* Journal of Cell Science 124.19 (2011): 3344–3355

27. Shriya Sahu *Interaction of Phospholipase Cβ1 with the promoter of RNA interference, C3PO and its functional consequences*. Stony Brook University 2016